Virology 442 (2013) 74–81

Contents lists available at SciVerse ScienceDirect

Virology

journal homepage: www.elsevier.com/locate/yviro

Negatively charged residues in the endodomain are critical for specific assembly of spike protein into murine coronavirus

Qianqian Yao [a], Paul S. Masters [b], Rong Ye [a,*]

[a] Department of Microbiology and Parasitology, School of Basic Medical Sciences, Fudan University, Shanghai 200032, China
[b] Wadsworth Center, New York State Department of Health, Albany, New York, USA

ARTICLE INFO

Article history:
Received 20 February 2013
Returned to author for revisions
1 April 2013
Accepted 1 April 2013
Available online 28 April 2013

Keywords:
Coronavirus
Spike glycoprotein
Assembly
Endodomain
Negatively charged residues

ABSTRACT

Coronavirus spike (S) protein assembles into virions via its carboxy-terminus, which is composed of a transmembrane domain and an endodomain. Here, the carboxy-terminal charge-rich motif in the endodomain was verified to be critical for the specificity of S assembly into mouse hepatitis virus (MHV). Recombinant MHVs exhibited a range of abilities to accommodate the homologous S endodomains from the betacoronaviruses bovine coronavirus and human SARS-associated coronavirus, the alphacoronavirus porcine transmissible gastroenteritis virus (TGEV), and the gammacoronavirus avian infectious bronchitis virus respectively. Interestingly, in TGEV endodomain chimeras the reverting mutations resulted in stronger S incorporation into virions, and a net gain of negatively charged residues in the charge-rich motif accounted for the improvement. Additionally, MHV S assembly could also be rescued by the acidic carboxy-terminal domain of the nucleocapsid protein. These results indicate an important role for negatively charged endodomain residues in the incorporation of MHV S protein into assembled virions.

Introduction

Coronaviruses are a family of enveloped, positive-sense single-stranded RNA viruses (Spaan et al., 2005). Since the first disease caused by a coronavirus, feline infectious peritonitis, was described one century ago, these viruses have come to be recognized as important pathogens that cause a variety of diseases in respiratory, digestive, and nervous systems of avian and mammalian hosts (Siddell, 1995). Before the identification of a new human coronavirus, severe acute respiratory syndrome-associated coronavirus (SARS-CoV) in 2003, there were only two known human coronaviruses, both associated with the common cold (Peiris et al., 2003; Lai, et al., 2007). In the past decade numerous new coronaviruses have been isolated, including three additional human coronaviruses and numerous previously unknown bat coronaviruses. A revised and updated taxonomy has divided the family into four genera—the alpha-, beta-, gamma-, and deltacoronaviruses (Adams and Carstens, 2012). The coronavirus spike (S) protein, a glycosylated class I viral fusion protein, is critical for viral infectivity, species and tissue tropism, and pathogenesis (Gallagher and Buchmeier, 2001). In many coronaviruses, including the prototype betacoronavirus mouse hepatitis virus (MHV), most S molecules incorporated into virions are cleaved by a cellular furin-like enzyme into two equal-sized subunits, S1 and S2 (de Haan et al., 2004). The receptor binding domain is located in the N-terminal subunit, S1, while components involved in membrane fusion, such as the fusion peptide and heptad repeats, are located in the ectodomain portion of the C-terminal subunit, S2 (Cavanagh, 1995; Holmes et al., 2001; Masters, 2006). The carboxy terminus of S is composed of a hydrophobic transmembrane (Tm) domain and a hydrophilic endodomain (Endo), and virus-like particle studies originally mapped to these two domains the ability of S protein to be recruited by the membrane (M) protein for virion assembly (de Haan et al., 1999, 2000; Godeke et al., 2000). Endo is further divided into two regions of roughly equal size: a membrane-proximal cysteine-rich motif and a carboxy-terminal charge-rich motif (Bos et al., 1995; Chang et al., 2000; Godeke et al., 2000). The cysteine-rich segment of Endo is the target for multiple modifications by S-palmitoylation. A minimum number of cysteine residues is required for viral viability (Yang et al., 2012), and the cysteine-rich motif appears to be principally required for cell–cell fusion (Bos et al., 1995; Chang et al., 2000; Ye et al., 2004; Petit et al., 2007; Shulla and Gallagher, 2009; McBride and Machamer, 2010a). The charge-rich motif, on the other hand, has been shown to be the major determinant for S protein incorporation into assembling virions (Ye et al., 2004; Bosch et al., 2005). However, some evidence also suggests an effect of the cysteine-rich motif on assembly (Thorp et al., 2006).

Targeted RNA recombination is a reverse genetics system for coronaviruses that has been efficiently used to study the interactions of coronavirus structural proteins (Masters and Rottier, 2005; Masters et al., 2006), as well as for the expression of foreign genes

* Correspondence to: Department of Microbiology and Parasitology, School of Basic Medical Sciences, Fudan University, 138 Yixueyuan Road, P.O. Box 115, Shanghai 200032, China. Fax: +86 21 54237220.
E-mail address: yerong24@fudan.edu.cn (R. Ye).

0042-6822/$ - see front matter © 2013 Published by Elsevier Inc.
http://dx.doi.org/10.1016/j.virol.2013.04.001

engineered to replace the nonessential genes 2 and 4 of MHV (Das Sarma et al., 2002; Hurst et al., 2005; Yang et al., 2011, 2012; Ye et al., 2004). We previously combined both of these properties to develop a method to dissect the Tm and Endo domains of S protein and to distinguish between the effects of mutations on the assembly of S into virions versus other functions of S (Ye et al., 2004). In this strategy, one set of recombinants was created in which mutations were introduced directly into the S protein Tm or Endo and their effects on virus viability and growth properties were evaluated (Fig. 1A). A second set of recombinants was also generated in which wild-type S protein remained unaltered, and the same mutations were moved into the Tm and Endo domains of a heterologous membrane protein, designated Hook (HK), which was expressed in place of the nonessential genes 2a/HE. HK is small (38-kDa), epitope-tagged synthetic protein composed of a signal peptide, ectodomain, Tm, and endodomain from various cellular sources (Chesnut et al., 1996; Ye et al., 2004). The effects of the mutations on the incorporation of HK protein into purified virions could then be directly assayed, independent of whether they had an impact on S protein (Fig. 1B).

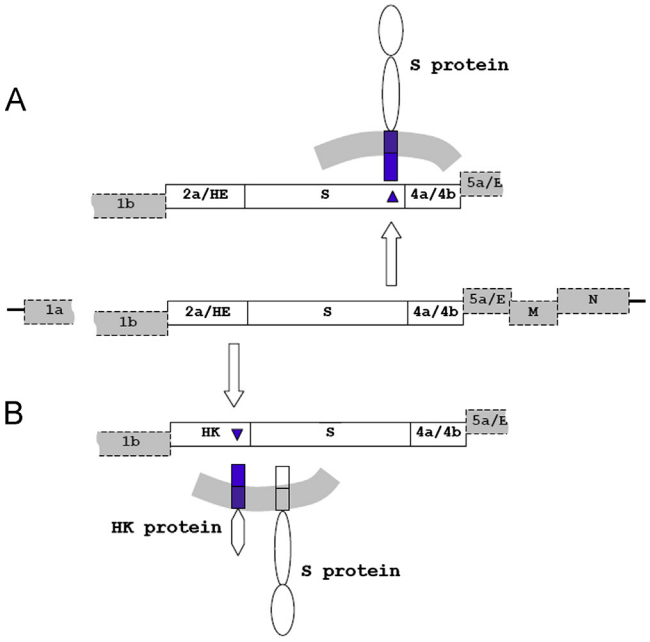

Fig. 1. Strategy to test S assembly by construction of MHV recombinants bearing mutated Tm and Endo domains. (A) The upper part of the diagram shows the introduction of mutations (blue triangle) into the S gene, resulting in production of S protein with mutated Tm and Endo domains (blue rectangles). (B) The lower part of the diagram shows the introduction of mutations (blue triangle) into the HK gene, which is substituted for the nonessential 2a/HE genes, resulting in production of HK protein with mutated Tm and Endo domains (blue rectangles), while the wild-type S gene and protein remain unaltered.

In the current study, we analyzed the effects of the Endo charge-rich motif on virion incorporation of MHV S protein through substitutions of the homologous regions from the alphacoronavirus porcine transmissible gastroenteritis virus (TGEV), the betacoronaviruses bovine coronavirus (BCoV) and SARS-CoV, or the gammacoronavirus avian infectious bronchitis virus (IBV). The results showed that the ability of recombinant MHVs to accommodate Tm and Endo domains from other virus species depended on their phylogenetic relatedness to MHV. Thus, the BCoV and SARS-CoV substitutions were completely allowed, while the TGEV substitution retained only partial functionality, and the IBV substitution was lethal. Further analysis of TGEV substitutions and revertants obtained there from revealed the importance of negatively charged Endo residues for the incorporation of MHV S protein into assembled virions. Finally, we were able to replace the MHV Endo charge-rich motif with the acidic carboxy-terminal domain of the nucleocapsid (N) protein.

A

Genus	Virus	Transmembrane Domain	Endodomain
β	MHV	-**WPWYVWLLIGLAGVAVCVLLFFI**--CCC-TGCGSCCFKK--CGNCCDEYGGHQDS-IVIHNISSHED*	
α	TGEV	-**WPWYVWLLIGLVVIFCIPLLLF**---CCCSTGCCGCIGCL---GSCCHSICSRRQFENYEPIEKVHVH*	
β	BCoV	-**WPWYVWLLIGFAGVAMLVLLFFI**--CCC-TGCGTSCFKI--CGGCCDDYTGHQE--LVI--KTSHDD*	
γ	IBV	-**WPWYVWLAIAFATIIFILILGWVFF**MTGCCGCCCGCFGIMPLMSKCGKKSSYYTTFDNDVVTEQYRPKKSV*	
β	SARS-CoV	-**WPWYVWLGFIAGLIAIVMVTILL**-CCMTSCCSCLKGACSCGSCCKFDEDDSEPVLKGVKLHYT*	

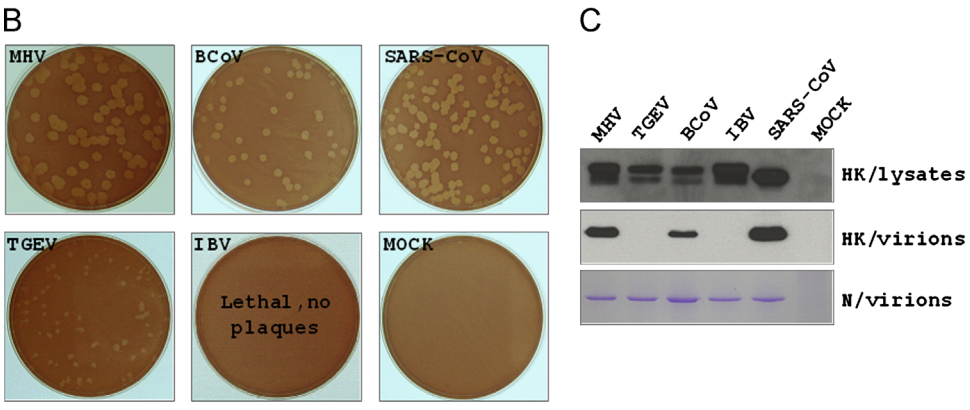

Fig. 2. Effects on assembly caused by the replacement of the C-terminus of MHV S protein with C-termini from different coronaviruses. (A) Alignment of C-terminal transmembrane domain (bold) and endodomain amino-acid sequences of the S proteins of alphacoronavirus TGEV (AJ271965), gammacoronavirus IBV (AJ311317), and betacoronaviruses MHV-A59 (AY700211), BCoV (U00735), and SARS-CoV Urbani (AY278741) (GenBank accession numbers given in parentheses). (B) Plaque assay of MHV S protein recombinants. The C-terminus of MHV S protein was replaced with the homologous sequence from TGEV, BCoV, IBV, or SARS-CoV. Mouse L2 cells were infected with recombinant viruses for 2 h, overlaid with agar for 40 h and then stained for 8 h with neutral red. Mock infection was conducted with sterile media. (C) Immunoblotting analysis of substituted HK proteins incorporated into MHV recombinant. Top panel, HK expressed by recombinant MHVs in 17Cl1 cells (lysates). Middle panel, HK incorporated into purified recombinant MHV virions. Bottom panel, N protein as a control for normalization of virions (Coomassie-stained). In the top and middle panels, HK was detected with mouse mAb to HA tag and HRP-conjugated goat anti-mouse IgG.

Results

Recombinant MHVs displayed a range of accommodations to different carboxy-terminal sequences from other coronavirus S proteins

There are currently some twenty to thirty species of coronaviruses, which are now classified into four genera (formerly groups), designated the alpha-, beta-, gamma-, and deltacoronaviruses (Adams and Carstens, 2012; Spaan et al., 2005). Although the S2 portions of coronavirus S proteins show some degree of conservation, the Tm and Endo domains are highly divergent, with the exception of a conserved cluster of seven hydrophobic residues (WPWYVWL) at the start of Tm. To evaluate the functionality of different C-terminal sequence motifs in the MHV S protein, we constructed two sets of mutants in which the ectodomain of either S protein or HK protein was fused to the Tm and Endo domains from TGEV (an alphacoronavirus), BCoV (a betacoronavirus), SARS-CoV (a betacoronavirus), or IBV (a gammacoronavirus) (Fig. 2A). Substitution of the C-terminal sequence from BCoV S did not significantly hinder the assembly of MHV S into virions. As shown in Fig. 2B, the chimeric S recombinant formed slightly smaller plaques than wild-type MHV. Correspondingly, the BCoV-substituted HK protein was incorporated into the virions at a lower level than the MHV version of HK protein (2B). More significant assembly was observed with the C-terminal replacement from SARS-CoV S. The chimeric S recombinant formed plaques similar in size and morphology to the MHV wild type, and much more SARS-CoV-substituted HK protein became incorporated into purified virions. By contrast, substitution of the C-terminal sequence from IBV S protein was lethal to recombinant MHV; consistent with this finding, IBV-substituted HK protein was not incorporated into purified virions. Intermediate between these extremes, an MHV S mutant containing the C-terminus of the TGEV S protein was markedly debilitated but viable. This recombinant had a much lower titer and formed smaller, heterogeneous plaques compared to those of wild-type MHV (larger plaques in Fig. 2B were later found to be revertants). However, there was no detectable incorporation of the TGEV-substituted HK protein into virions. In general, the toleration of MHV S protein for replacement of its Tm and Endo domains by the homologous regions of other S proteins was highest within the same genus (betacoronaviruses) and marginal for the somewhat more closely related alphavirus genus. A substitution originating from the more distantly related gammacoronavirus genus was unallowed.

Charge-rich motif in the endodomain plays a key role in S assembly

We previously demonstrated, through the construction of deletion and point mutations, that the charge-rich motif of Endo has a dominant role in the incorporation of S protein into virions (Ye et al., 2004). We thus hypothesized that this motif might be the critical element allowing or precluding the substitution of C-termini from other coronavirus S proteins in place of that of MHV. To test this notion, we constructed two groups of recombinant MHVs with chimeric C-terminal sequences (Fig. 3A), in each case as separate S protein and HK protein mutants. In Mut-SSM and Mut-TTM, the Tm and the cysteine-rich motif were from SARS-CoV S or TGEV S, respectively, while the charge-rich motif was from MHV S. In Mut-MMS and Mut-MMT, the Tm and the cysteine-rich motif were from MHV S, and the charge-rich motif was from either SARS-CoV S or TGEV S, respectively. For negative controls, we used the truncation mutant Mut-30 (mutant Δ20 in Ye et al., 2004), which essentially lacks the entire MHV charge-rich motif. Mut-30 is minimally viable as an S protein mutant and its HK protein counterpart fails to be incorporated into virions. As we anticipated, recombinants bearing the charge-rich motif of MHV S (Mut-SSM and Mut-TTM) or the charge-rich motif of

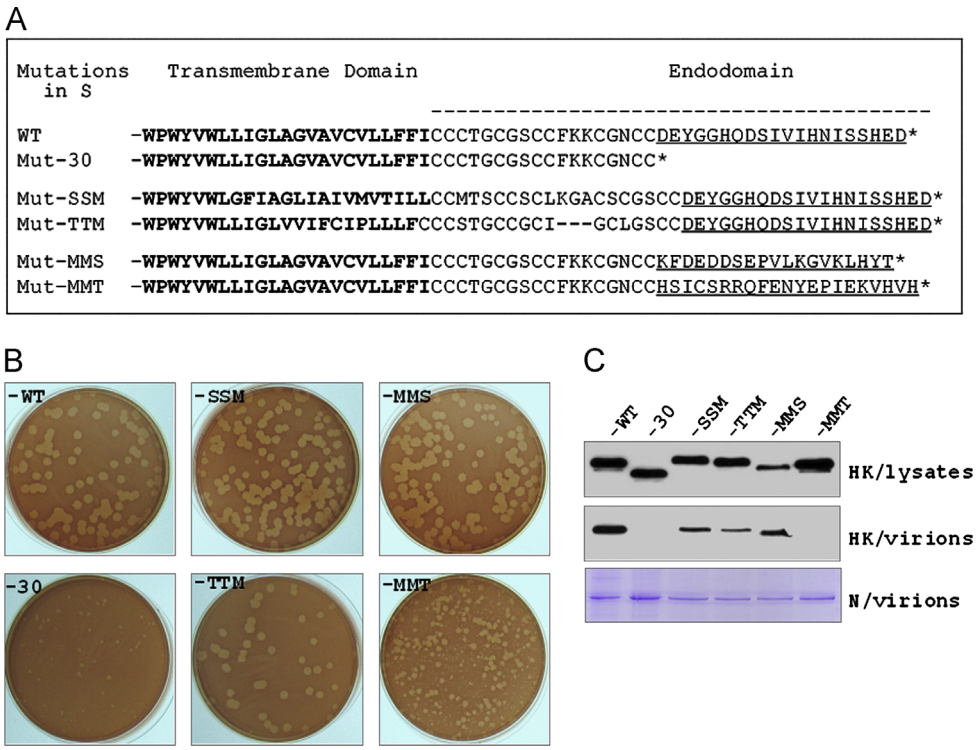

Fig. 3. Dominant role of the charge-rich motif in S assembly. (A) Amino acid sequences of the chimeric C-termini in S or HK MHV recombinants. Tm are shown in bold and Endo are divided into the cysteine-rich motif and the charge-rich motif (underlined). The upper two sequences are from wild-type S (WT) or a charged-rich motif-truncated mutant (Mut-30). In the remaining four chimeric mutant sequences, the first, second, and third letters represent the source (MHV, SARS-CoV, or TGEV) of the Tm, cysteine-rich motif, and charge-rich motif, respectively. Plaque assays of recombinant MHV S protein mutants and immunoblotting analysis of mutant HK proteins incorporated into recombinant virions are shown in panels (B) and (C), as described in Fig. 2.

SARS-CoV (Mut-MMS) produced wild type-like plaques (Fig. 3B) and their corresponding HK proteins were incorporated into virions (Fig. 3C), irrespective of the source of their Tm and cysteine-rich motifs. Conversely, the S protein recombinant containing the TGEV charge-rich motif (Mut-MMT) produced tiny and irregular plaques (Fig. 3B) that were similar to the mutant with the entire C-terminus of TGEV S (Fig. 2B), despite that fact that both the Tm and cysteine-rich motif of Mut-MMT were derived from MHV S. Moreover, the Mut-MMT HK protein exhibited no incorporation into virions (Fig. 3C). These results confirmed that the charge-rich motif in endodomain plays a more important role in the specific assembly of MHV S into virions than does the Tm domain or the cysteine-rich motif.

Reverting mutations in TGEV chimeras improved S assembly by eliminating positively charged residues in the endodomain

MHV S protein mutants containing the entire carboxy terminus or just the charge-rich motif of TGEV S (Mut-TGEV and Mut-MMT) produced irregular plaques (Figs. 2B, 3B, 4A). Most of these plaques were very small and morphologically similar to those produced by the C-terminal truncation mutant, Mut-30 (Ye et al., 2004). Larger plaques arose following multiple passages of the TGEV chimeric mutants, while plaques produced by Mut-30 maintained a stable small morphology after passage under the same conditions. A number of larger plaques were randomly picked and subjected to multiple rounds of plaque purification, during which their large-plaque morphology remained stable (Fig. 4A). RT-PCR and sequencing analyses of the relevant segment of the S gene and downstream genes showed that each of the isolated revertants had acquired a deletion in Endo (Fig. 4B). Moreover, the observed deletions fell into two classes. In one class (revertants TGEV-R1 and MMT-R1), the charge-rich motif of TGEV S was totally deleted, and a new carboxy-terminal sequence of seven residues, TENLNNL, was created through juxtaposition of a normally untranslated open reading frame beginning 24 nucleotides downstream of the S gene. In the second class (revertants TGEV-R2 and MMT-R2), the TGEV S protein carboxy terminus was retained, but a portion of the charge-rich motif containing two adjacent positively-charged arginine residues was deleted. No other mutations were observed in these revertants in the S Tm domain or in the structural proteins E, M, or N (data not shown).

Significantly, these reverting mutations displayed a tendency to delete positively-charged residues, either two arginines (RR) from the charge-rich motif of TGEV S or two lysines (KK) from the cysteine-rich motif of MHV S (Fig. 4B). This suggested that positively-charged residues in those positions were harmful to the assembly of MHV S. Additionally, the heptapeptide TENLNNL, created by two of the reverting mutations, introduced one negatively-charged glutamic acid (E) plus four polar residues (T and N) that might be beneficial to the assembly of S.

To directly test the role of the heptapeptide TENLNNL in MHV S protein incorporation, three further sets of mutants were generated (Fig. 5A). Mut-70 was designed to reconstruct the revertant MMT- R1. Mut-69 was a mimic of revertant MMT-R1, but did not contain the heptapeptide. Finally, Mut-71 maintained just three residues (TEN) of the heptapeptide, to check the importance of the negatively-charged E residue. The chimeric S recombinant of Mut-70 formed homogenous plaques (Fig. 5B) whose morphology and size relative to the wild type was very similar to that of revertant MTT-R1 (Fig. 4A). In accord with this, the Mut-70 HK protein was incorporated into virions almost as well as wild-type HK protein (Fig. 5C). This confirmed that the identified deletion in revertant MTT-R1 was indeed responsible for its observed gain of S protein function.

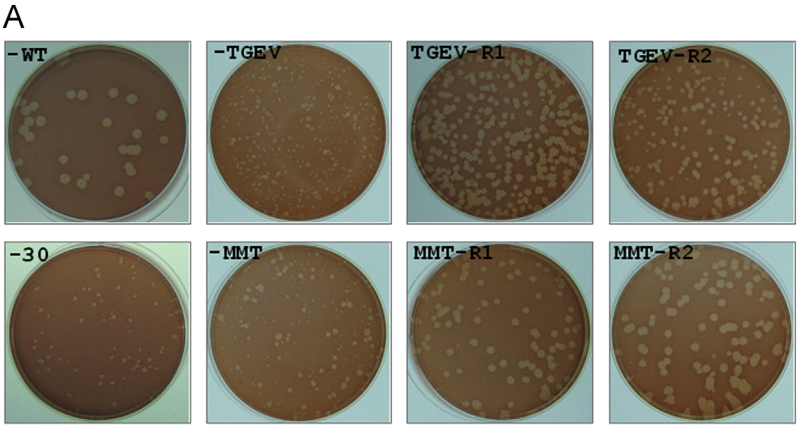

B

```
Mutations  Transmembrane Domain                    Endodomain
   in S
                                  ------------------------------------
WT        -WPWYVWLLIGLAGVAVCVLLFFICCCTGCGSCCFKKCGNCCDEYGGHQDSIVIHNISSHED*
Mut-30    -WPWYVWLLIGLAGVAVCVLLFFICCCTGCGSCCFKKCGNCC*

Mut-TGEV  -WPWYVWLLIGLVVIFCIPLLLF-CCCSTGCCGCIGCLGSCCHSICSRRQFENYEPIEKVHVH*
TGEV-R1   -WPWYVWLLIGLVVIFCIPLLLF-CCCSTGCCGCIGCLGSCCHSICS---TENLNNL*
TGEV-R2   -WPWYVWLLIGLVVIFCIPLLLF-CCCSTGCCGCIGCLGSCCHSI----QFENYEPIEKVHVH*

Mut-MMT   -WPWYVWLLIGLAGVAVCVLLFFICCCTGCGSCCFKKCGNCCHSICSRRQFENYEPIEKVHVH*
MMT-R1    -WPWYVWLLIGLAGVAVCVLLFFICCCTGCGSCCF---------------TENLNNL*
MMT-R2    -WPWYVWLLIGLAGVAVCVLLFFICCCTGCGSCCFKKCGNCC----------YEPIEKVHVH*
```

Fig. 4. Reverting mutations arising in TGEV chimeric S proteins. (A) Plaque assay of the original TGEV S protein Endo recombinants (Mut-TGEV and Mut-MMT) and their corresponding purified revertants (TGEV-R1, TGEV-R2, MMT-R1, and MMT-R2); wild-type (WT) and Mut-30 viruses served as positive and negative controls, respectively. (B) Alignment of mutated Endo sequences of revertants compared to their parents and controls; the newly generated heptapeptide terminus of TGEV-R1 and MMT-R1 is underlined.

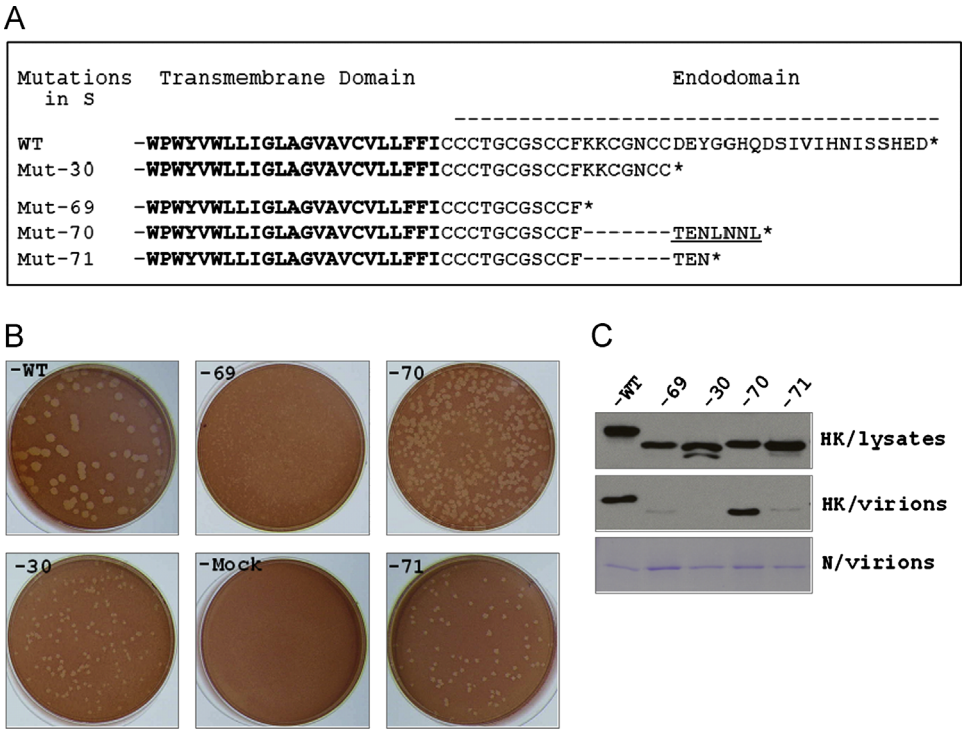

Fig. 5. The charged-rich motif produced by the MMT-R1 reverting mutation restored S assembly into virions. (A) Alignment of C-terminal sequences of S or HK MHV recombinants with reverting mutations. Mut-70 and Mut-71 were constructed with sequences from reverting mutant MMT-R1. WT and two terminally-truncated mutants (Mut-69 and Mut-30) served as controls. Tm are shown in bold, and the heptapeptide TENLNNL is underlined. Plaque assays of recombinant MHV S protein mutants and immunoblotting analysis of mutant HK proteins incorporated into recombinant virions are shown in panels (B) and (C), as described in Fig. 2.

The chimeric S recombinant of Mut-71 produced plaques that were smaller than those of Mut-70 but were still larger and clearer than those of the Mut-69 S-mutant control (Fig. 5B). However, both the Mut-71 and Mut-69 HK proteins displayed weak incorporation into virions (Fig. 5C). Thus, the tripeptide TEN is not sufficient to fully recapitulate the advantage conferred by the heptapeptide TENLNNL. Curiously, the weak incorporation into virions of Mut-69 HK protein was still stronger than the consistently undetectable incorporation of Mut-30 HK protein, despite the fact that the Mut-30 endodomain was 7 residues longer than that of Mut-69. We speculate that, in the absence of multiple negatively charged residues elsewhere in Endo, the deletion of two adjacent positively-charged lysines (KK) in Mut-69 removed a charge and spatial hindrance, thereby allowing some limited enhancement of S (or HK) protein incorporation into virions.

MHV N protein domain 3 partially rescued S assembly

The coronavirus M protein is the central organizer of virion assembly and budding through interactions that it carries out with both the S and the N proteins (Masters, 2006). M-S interactions encompass the carboxy-terminal endodomain of M protein but do not involve the extreme carboxy terminus of M protein (de Haan et al., 1999; McBride and Machamer, 2010b). Conversely, M–N interactions are predominantly or solely mediated by the extreme carboxy terminus of M protein and the carboxy-terminal domain 3 of N protein (Kuo and Masters, 2002; Hurst et al., 2005; Verma et al., 2007; Hurst et al., 2010). To determine if it was possible to replace the M-interacting region of the S protein with the M-interacting region of the N protein, we created S protein and HK protein mutants in which the charge-rich motif was replaced with MHV N protein domain 3 (Mut-MN) (Fig. 6A). We also made recombinants substituting the related domain 3 of the BCoV N protein (Mut-BN) or else the short endodomain of the MHV hemagglutinin-esterase (HE) protein (Mut-HE). HE is a membrane envelope structural protein that is expressed in a subset of betacoronaviruses (Lissenberg et al., 2005); the M-interacting region of HE has not been mapped.

The chimeric S recombinant of Mut-MN formed plaques that were smaller than those of the wild type but slightly larger than those of Mut-BN or Mut-HE (Fig. 6B). The Mut-MN HK protein displayed weaker incorporation into virions than wild-type or Mut-70 HK protein, but incorporation of Mut-MN HK protein was substantially stronger than that of Mut-BN HK protein (Fig. 6C). From these results we conclude that the MHV N protein domain 3 could partially function to replace the S protein endodomain charge-rich motif. However, it is unlikely that this transplanted N domain 3 appropriated the normal M-N interaction, since the BCoV domain 3 in Mut-BN was unable to play the same role. In the MHV M-N interaction, domain 3 of BCoV N protein is entirely functionally interchangeable with its MHV counterpart (Hurst et al., 2010). Additionally, our results show that the HE protein endodomain could not replace the S protein charge-rich motif.

Discussion

The coronavirus S protein is the largest described class I viral fusion protein, comprising as many as 1450 amino acid residues. Its ectodomain, which contains the elements of receptor recognition and membrane fusion, accounts for almost the entirely of the protein. A small Tm domain and Endo region, at most some 70 amino acid residues, governs membrane anchoring and incorporation of S into virions. At the boundary between these two regions, either proximal to, or within the outer leaflet of the membrane, there is a cluster of 7 aromatic hydrophobic residues (WPWYVWL) that is highly conserved among all coronaviruses (Bos et al., 1995; Sainz et al., 2005). In contrast to this conservation, many of the other parts of S protein show considerable divergence, both across genus boundaries and even within a given genus.

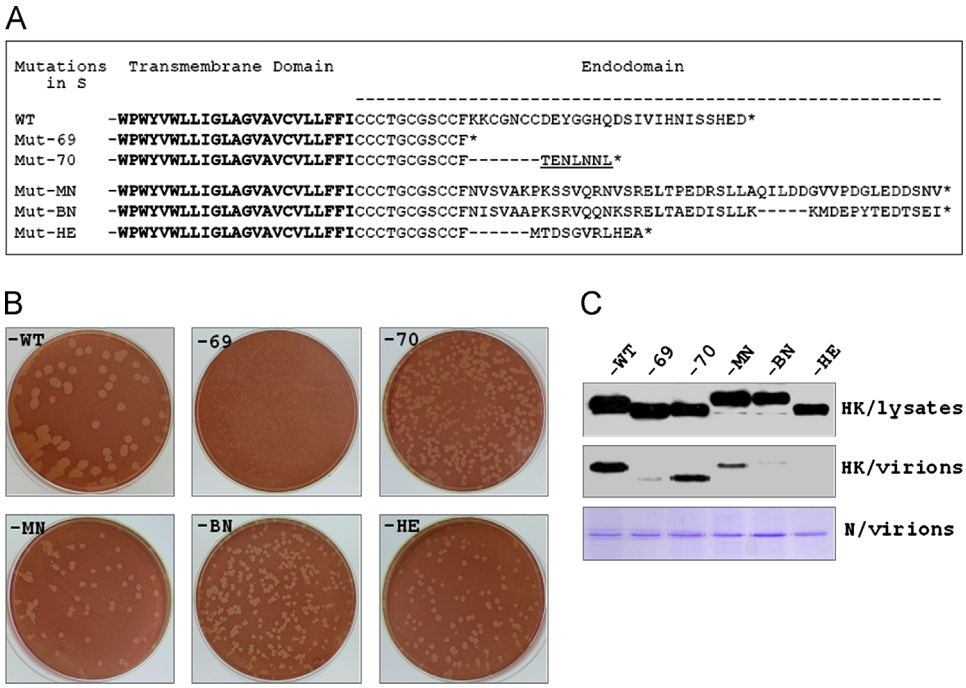

Fig. 6. N protein domain 3 could partially rescue S assembly into virions. (A) Alignment of C-terminal sequences of S or HK MHV recombinants in which the charge-rich motif was replaced with N protein domain 3 from either MHV (Mut-MN) or BCoV (Mut-BN), or else with HE Endo (Mut-HE). WT, truncated mutant (Mut-69), and MMT-R1 mimicking mutant (Mut-70) served as controls. Tm are shown in bold, and the heptapeptide TENLNNL is underlined. Plaque assays of recombinant MHV S protein mutants and immunoblotting analysis of mutant HK proteins incorporated into recombinant virions are shown in panels (B) and (C), as described in Fig. 2.

The functional division between the S protein ectodomain and the Tm plus Endo was first demonstrated in virus-like particle studies (Godeke et al., 2000). It was later shown that exchanging the S ectodomain at the WPWYVWL motif could switch the species specificity of coronaviruses, provided that the native transmembrane domain and endodomain were retained. This served as the basis to establish a strong host-range-based selection for targeted RNA recombination as a reverse genetics system (Kuo et al., 2000; Haijema et al., 2003). We have used this system to dissect the requirements for S incorporation into virions through construction of mutations in the MHV S protein Tm plus Endo region. Since such mutational alteration of S may possibly affect S maturation, trafficking, or membrane fusion, we also constructed the same mutations in an epitope-tagged artificial membrane protein, HK, which was derived from heterologous components (originally in pHook1, Chesnut et al., 1996). This strategy previously allowed us to map the assembly competence of S to Endo (Ye et al., 2004), a conclusion also reached by others (Bosch et al., 2005).

In the present work, we further probed S protein incorporation by engineering interspecies chimeras in which the Tm and Endo segments of MHV S were replaced with those of closely or distantly related coronaviruses. We observed that these domains taken from the betacoronaviruses BCoV and SARS-CoV could readily substitute for their MHV counterparts (Fig. 2). The functionality of the BCoV components in MHV is not surprising, given the generally high sequence homology between many proteins of these two viruses, and the interchangeability of other domains between them (Masters et al., 2006; Hurst et al., 2010). The ability of the SARS-CoV S protein Tm and Endo to operate in MHV further underscores the phylogenetic relatedness of these two viruses. Although initial characterizations of SARS-CoV placed it in a unique grouping, it has since become firmly established that this virus falls in the betacoronaviruses and that MHV and BCoV are among its closer relatives (Snijder et al., 2003; Weiss and Navas-Martin, 2005). S protein Tm and Endo domains derived from other genera of the coronavirus family were much less effective in MHV S. The most far-reaching substitution, that of IBV, was lethal. The TGEV substitution, however, was marginally functional. Construction of additional chimeras within the Tm plus Endo region more finely mapped the major determinant of virion incorporation to the charge-rich motif of Endo (Fig. 3), consistent with our previous results (Ye et al., 2004).

Examination of allowed and unallowed substitutions suggested that the number and location of negatively-charged residues in the charge-rich motif was critical for S protein incorporation into virions. Additional work provided strong support for this surmise. First, we were able to obtain revertants of TGEV chimeras that restored some of the functionality of the chimeric Endo segments. Analysis of these mutants showed that the quality they had in common was the gain of negatively-charged residues and the loss of positively-charged residues in the charge-rich motif (Figs. 4 and 5). Second, replacement of the charge-rich motif of S protein with the acidic carboxy-terminal domain 3 of the MHV N protein at least partially restored Endo function (Fig. 6). The evidence suggests that this came about through mimicking the essential attributes of the charge-rich motif and not through the interaction that N domain 3 normally makes with the extreme carboxy terminus of M protein. The BCoV N domain 3 was unable to replace the Endo charge-rich motif of MHV S, even though BCoV N domain 3 is completely active as a replacement for the MHV N domain 3 (Hurst et al., 2010). The region of the MHV M endodomain that interacts with S protein has been previously localized to be upstream of the extreme carboxy terminus of M (de Haan et al., 1999). Our data suggests that this S-interacting surface must have one or more key positively-charged residues that contact the negatively-charged charge-rich motif of the MHV S Endo. It also appears that endodomain interactions with M protein are not the sole means by which viral membrane proteins can partition into assembling virions. The failure of the Mut-HE mutant to become incorporated into virions suggests that there exist other types of interactions that lead to the effective inclusion of HE protein in the

viral envelope. Additionally, it is possible that the constraints on S protein endodomain composition reflect its more complex range of interactions with membranes. Thus, a charge-rich region of a certain length may be uniquely required by S protein for virion assembly, in order to counterbalance the properties of other elements required for the fusion function of S, such as the WPWYVWL motif and the cysteine-rich motif. The M protein endodomain has thus far been resistant to structural determination. Thus, there is a large gap in our understanding of the complexity of its interactions with multiple proteins, including other molecules of M. The identification and characterization of all M protein interactions within the coronavirus virion remains an important future challenge.

Material and methods

Cells and viruses

Mouse 17 Clone 1 (17Cl1) cells were used for propagation of wild-type MHV-A59 and recombinant MHVs. Mouse fibroblast L2 cells were used for plaque assays and plaque purification of wild-type and recombinant MHVs. Felis catus whole fetus cells (FCWF) were used to grow the interspecies chimeric virus fMHV.v2 in which the ectodomain of the S gene of MHV is replaced with that of FIPV (Goebel, et al., 2004; Kuo, et al., 2000). The three cell lines were cultured in DMEM (GIBCO, Invitrogen) supplemented with 10% FBS and 0.37% sodium bicarbonate in a humidified 5% CO_2 atmosphere at 37 °C.

Plasmid construction

For the generation of recombinants in which mutations were introduced directly into the S protein Tm and Endo region, donor RNA transcription vectors were derived from plasmid pMH54 (Kuo et al., 2000). DNA fragments with deletion or replacement mutations were created as described previously (Yang et al., 2011; Ye et al., 2004) using primer-pair PCR and splicing overlap extension PCR. Mutated fragments were then transferred to pMH54 by replacement of the unique MluI-SbfI fragment running from the S ectodomain to the intergenic region downstream of S. For the generation of recombinants in which mutations were introduced into the HK protein Tm and Endo region, donor RNA transcription vectors were derived from the previously described vector pHKP1 (Ye et al., 2004). The pMH54-derived plasmids were used as the templates for the amplification of PCR fragments of the mutated Tm and Endo regions, which were then used to replace the unique SalI-AscI fragment of pHKP1 that contains the HK protein Tm and Endo region. All constructs were identified by restriction digest analysis, and cloning sites and junctions in plasmids were confirmed by sequencing.

Production of MHV recombinants

MHV mutants were produced by targeted RNA recombination (Masters and Rottier, 2005). Briefly, FCWF cells were infected with fMHV and digested with trypsin at 2 h post-infection (hpi) and washed twice with Mg^{++}- and Ca^{++}-free PBS. For preparation of donor RNA transcription, the constructed pMH54 or pHKM plasmids were digested with PacI and transcribed into mRNA using mMESSAGE mMACHINE T7 Ultra kit (Ambion). Approximately 10 μl of each recombinant transcript was used for transfection of ~10^7 infected FCWF cells. RNA transfection was performed using a Gene Pulser XceII electroporation system (Bio-Rad), with one pulse at settings of 975 μF and 0.3 kV. The co-transfected FCWF cells were loaded onto L2 monolayers grown in 6-well plates. Cytopathic effects were monitored and the supernatants were collected at 24, 48, and 72 hpi. Recombinant MHVs were purified by two rounds of plaque purification on L2 cells, and all mutations were verified by RT-PCR and sequencing.

Plaque assay

L2 cells were grown in 60-mm dishes to 70–80% confluence and infected with 1 ml of media containing viruses at dilutions ranging from 10^{-3} to 10^{-6}. Seven ml of 0.95% agar (Amresco) in DMEM with 5% FBS was overlaid onto cells at 2 hpi. Plaques were picked between 48 and 72 hpi. For plaque staining, 3 ml of agar with 0.02% neutral red (Sigma-Aldrich) was overlaid onto cells. Six to eight hours later, the stained plaques were counted or photographed using a white light transilluminator (Upland).

Virion purification

MHV recombinants expressing wild-type and mutant HK proteins were purified as described previously (Ye et al., 2004). Briefly, viral supernatants were precipitated by polyethylene glycol, and resuspended virus was isolated through two cycles of gradient centrifugation with 0 to 50% potassium tartrate contrasting 30 to 0% glycerol in TME buffer (50 mM Tris-maleate, pH 6.5 and 1 mM EDTA). Gradients were centrifuged at 111,000 × *g* in a Beckman SW41 rotor at 4 °C for 16–24 h. After centrifugation, viral bands were collected from the gradients and diluted with TME with 100 mM NaCl. Virions were pelleted through a glycerol cushion by centrifugation for 2 h at 151,000 × *g* and resuspended in PBS.

SDS-PAGE and western blotting

Infected 17Cl1 cells were washed twice with ice-cold PBS and collected in IPP buffer (50 mM Tris–HCl, pH 8.0, 150 mM NaCl, 1.0% Nonidet P-40) containing completeR protease inhibitor cocktail (Roche). Cell lysates were incubated on ice for 5 min and clarified by centrifuging at 12,000 × *g* for 5 min at 4 °C. Protein samples from either lysates or purified virions were mixed with an equal volume of 2 × sample buffer and heated at 95 °C for 5 min. One set of cell lysates and two identical sets of purified virions samples were separated by SDS-polyacrylamide gel electrophoresis. After electrophoresis, one gel with a set of purified virions was stained with Coomassie blue to illustrate N protein. Another gel with a set of purified virions and the gel with cell lysates were transferred onto PVDF membranes using a Criterion Blotter (Bio-Rad). Membranes were blocked for 1 h in 5% non-fat milk and incubated with 0.4 μg/ml mouse mAb to HA tag (Roche) overnight at 4 °C, followed by incubation with horseradish peroxidase-conjugated secondary antibody (GE, Amersham). The signal was developed using ECL system (GE, Amersham).

Acknowledgments

This study was supported in part by grants from the National Institutes of Health (National Institute of Allergy and Infectious Diseases), USA (R01 AI064603—P.S.M.) and the National Natural Science Foundation, China (31170786—R.Y.).

References

Adams, M.J., Carstens, E.B., 2012. Ratification vote on taxonomic proposals to the International Committee on Taxonomy of Viruses (2012). Arch. Virol. 157, 1411–1422.

Bos, E.C., Heijnen, L., Luytjes, W., Spaan, W.J., 1995. Mutational analysis of the murine coronavirus spike protein: effect on cell-to-cell fusion. Virology 214, 453–463.
Bosch, B.J., de Haan, C.A., Smits, S.L., Rottier, P.J.M., 2005. Spike protein assembly into the coronavirion: Exploring the limits of its sequence requirements. Virology 334, 306–318.
Cavanagh, D., 1995. The coronavirus surface glycoprotein. In: Siddell, S.D. (Ed.), The Coronaviridae. Plenum Press, New York, NY.
Chang, K.W., Sheng, Y., Gombold, J.L., 2000. Coronavirus-induced membrane fusion requires the cysteine-rich domain in the spike protein. Virology 269, 212–224.
Chesnut, J.D., Baytan, A.R., Russell, M., Chang, M.P., Bernard, A., Maxwell, I.H., Hoeffler, J.P., 1996. Selective isolation of transiently transfected cells from a mammalian cell population with vectors expressing a membrane anchored single-chain antibody. J. Immunol. Methods 193, 17–27.
Das Sarma, J., Scheen, E., Seo, S.H., Koval, M., Weiss, S.R., 2002. Enhanced green fluorescent protein expression may be used to monitor murine coronavirus spread in vitro and in the mouse central nervous system. J. Neurovirol. 8, 381–391.
de Haan, C.A., Smeets, M., Vernooij, F., Vennema, H., Rottier, P.J., 1999. Mapping of the coronavirus membrane protein domains involved in interaction with the spike protein. J. Virol. 73, 7441–7452.
de Haan, C.A., Stadler, K., Godeke, G.J., Bosch, B.J., Rottier, P.J., 2004. Cleavage inhibition of the murine coronavirus spike protein by a furin-like enzyme affects cell–cell but not virus-cell fusion. J. Virol. 78, 6048–6054.
de Haan, C.A., Vennema, H., Rottier, P.J., 2000. Assembly of the coronavirus envelope: homotypic interactions between the M proteins. J. Virol. 74, 4967–4978.
Gallagher, T.M., Buchmeier, M.J., 2001. Coronavirus spike proteins in viral entry and pathogenesis. Virology 279, 371–374.
Godeke, G.J., de Haan, C.A., Rossen, J.W., Vennema, H., Rottier, P.J., 2000. Assembly of spikes into coronavirus particles is mediated by the carboxy-terminal domain of the spike protein. J. Virol. 74, 1566–1571.
Goebel, S.J., Hsue, B., Dombrowski, T.F., Masters, P.S., 2004. Characterization of the RNA components of a putative molecular switch in the 3′ untranslated region of the murine coronavirus genome. J. Virol. 78, 669–682.
Haijema, B.J., Volders, H., Rottier, P.J.M., 2003. Switching species tropism: an effective way to manipulate the feline coronavirus genome. J. Virol. 77, 4528–4538.
Holmes, K.V., Zelus, B.D., Schickli, J.H., Weiss, S.R., 2001. Receptor specificity and receptor-induced conformational changes in mouse hepatitis virus spike glycoprotein. Adv. Exp. Med. Biol. 494, 173–181.
Hurst, K.R., Kuo, L., Koetzner, C.A., Ye, R., Hsue, B., Masters, P.S., 2005. A major determinant for membrane protein interaction localizes to the carboxy-terminal domain of the mouse coronavirus nucleocapsid protein. J. Virol. 79, 13285–13297.
Hurst, K.R., Ye, R., Goebel, S.J., Jayaraman, P., Masters, P.S., 2010. An interaction between the nucleocapsid protein and a component of the replicase-transcriptase complex is crucial for the infectivity of coronavirus genomic RNA. J. Virol. 84, 10276–10288.
Kuo, L., Godeke, G.J., Raamsman, M.J., Masters, P.S., Rottier, P.J., 2000. Retargeting of coronavirus by substitution of the spike glycoprotein ectodomain: crossing the host cell species barrier. J. Virol. 74, 1393–1406.
Kuo, L., Masters, P.S., 2002. Genetic evidence for a structural interaction between the carboxy termini of the membrane and nucleocapsid proteins of mouse hepatitis virus. J. Virol. 76, 4987–4999.
Lai, M.M.C., Perlman, S., Anderson, L.J., 2007. Coronaviridae. In: Knipe, D.M., Howley, P.M., Griffin, D.E., Lamb, R.A., Martin, M.A., Roizman, B., Straus, S.E. (Eds.), Fields Virology, 5th ed. Lippincott Williams & Wilkins, Philadelphia, PA.
Lissenberg, A., Vrolijk, M.M., van Vliet, A.L.W., Langereis, M.A., de Groot-Mijnes, J.D. F., Rottier, P.J.M., de Groot, R.J., 2005. Luxury at a cost? Recombinant mouse hepatitis viruses expressing the accessory hemagglutinin-esterase protein display reduced fitness in vitro. J. Virol. 79, 15054–15063.
Masters, P.S., 2006. The molecular biology of coronaviruses. Adv. Virus Res. 66, 193–292.
Masters, P.S., Kuo, L., Ye, R., Hurst, K.R., Koetzner, C.A., Hsue, B., 2006. Genetic and molecular biological analysis of protein-protein interactions in coronavirus assembly. Adv. Exp. Med. Biol. 581 (III), 163–173.
Masters, P.S., Rottier, P.J., 2005. Coronavirus reverse genetics by targeted RNA recombination. Curr. Top. Microbiol. Immunol. 287, 133–159.
McBride, C.E., Machamer, C.E., 2010a. Palmitoylation of SARS-CoV S protein is necessary for partitioning into detergent-resistant membranes and cell-cell fusion but not interaction with M protein. Virology 405, 139–148.
McBride, C.E., Machamer, C.E., 2010b. A single tyrosine in the severe acute respiratory syndrome coronavirus membrane protein cytoplasmic tail is important for efficient interaction with spike protein. J. Virol. 84, 1891–1901.
Peiris, J.S., Lai, S.T., Poon, L.L., Guan, Y., Yam, L.Y., Lim, W., Nicholls, J., Yee, W.K., Yan, W.W., Cheung, M.T., Cheng, V.C., Chan, K.H., Tsang, D.N., Yung, R.W., Ng, T.K., Yuen, K.Y., 2003. Coronavirus as a possible cause of severe acute respiratory syndrome. Lancet 361, 1319–1325.
Petit, C.M., Chouljenko, V.N., Iyer, A., Colgrove, R., Farzan, M., Knipe, D.M., Kousoulas, K.G., 2007. Palmitoylation of the cysteine-rich endodomain of the SARS-coronavirus spike glycoprotein is important for spike-mediated cell fusion. Virology 360, 264–274.
Sainz Jr., B., Rausch, J.M., Gallagher, W.R., Garry, R.F., Wimley, W.C., 2005. The aromatic domain of the coronavirus class I viral fusion protein induces membrane permeabilization: putative role during viral entry. Biochemistry 44, 947–958.
Shulla, A., Gallagher, T., 2009. Role of spike protein endodomains in regulating coronavirus entry. J Biol. Chem. 284, 32725–32734.
Siddell, S.G., 1995. The Coronaviridae. Plenum Press, New York, NY.
Snijder, E.J., Bredenbeek, P.J., Dobbe, J.C., Thiel, V., Ziebuhr, J., Poon, L.L., Guan, Y., Rozanov, M., Spaan, W.J., Gorbalenya, A.E., 2003. Unique and conserved features of genome and proteome of SARS-coronavirus, an early split-off from the coronavirus group 2 lineage. J. Mol. Biol. 331, 991–1004.
Spaan, W., Cananagh, D., de Groot, R., Enjuanes, L., Snijder, E., Walker, P., 2005. Order Nidovirales. In: Fauquet, C.M., Mayo, M.A., Maniloff, J., Desselberger, U., Ball, L.A. (Eds.), Virus Taxonomy: Classification and Nomenclature of Viruses: Eighth Report of the International Committee on Taxonomy of Viruses. Elsevier Academic Press, San Diego, CA, pp. 937–945.
Thorp, E.B., Boscarino, J.A., Logan, H.L., Goletz, J.T., Gallagher, T.M., 2006. Palmitoylations on murine coronavirus spike proteins are essential for virion assembly and infectivity. J. Virol. 80, 1280–1289.
Verma, S., Lopez, L.A., Bednar, V., Hogue, B.G., 2007. Importance of the penultimate positive charge in mouse hepatitis coronavirus A59 membrane protein. J. Virol. 81, 5339–5348.
Weiss, S.R., Navas-Martin, S., 2005. Coronavirus pathogenesis and the emerging pathogen severe acute respiratory syndrome coronavirus. Microbiol. Mol. Biol. Rev. 69, 635–664.
Yang, J., Lv, J., Wang, Y., Gao, S., Yao, Q., Qu, D., Ye, R., 2012. Replication of murine coronavirus requires multiple cysteines in the endodomain of spike protein. Virology 427, 98–106.
Yang, J., Sun, Z., Wang, Y., Lv, J., Qu, D., Ye, R., 2011. Partial deletion in the spike endodomain of mouse hepatitis virus decreases the cytopathic effect but maintains foreign protein expression in infected cells. J. Virol. Methods 172, 46–53.
Ye, R., Montalto-Morrison, C., Masters, P.S., 2004. Genetic analysis of determinants for spike glycoprotein assembly into murine coronavirus virions: distinct roles for charge-rich and cysteine-rich regions of the endodomain. J. Virol. 78, 9904–9917.